

Figure 3: Schematic of a cryomodule for SRILAC.

into account the unloaded Q-factor (Q_0) of the resonator, actual beam loading, the strength of microphonics, and RF control. The coupling strength of the FPC is tunable by sliding in the azimuthal direction and tuning can be made without warming up the cold mass or breaking the vacuum of the cryostat chamber.

Instead of superconducting solenoids, room temperature quadrupole doublets are chosen to allow simple operation and alignment. Details of the design study for the SC-LINAC section, specifically, configuration of the accelerating resonators and quadrupoles and geometrical optimization of the QWRs, have been described elsewhere [7, 8].

DESIGN STUDIES FOR SC-QWRs FOR THE RIKEN SC-LINAC

Resonator

Details of the former design of the resonator were reported in Ref. [7]. Further optimization of the geometrical design was performed with the 3-D simulation software package CST Microwave Studio (MWS) [9]. By modifying the stem to a conical shape (instead of the original straight cylindrical shape) and making the inner diameter of the resonator larger, as shown in Fig. 4, the distribution of the magnetic field strength along the stem surface was flattened and, as a result, the peak magnetic field was greatly reduced. Its RF power dissipation was also reduced by 20%. The characteristics of the resonator are summarized in Table 1. For the estimation of Q_0 , an R_s ($\equiv R_{BCS} + R_{res}$) of 25 n Ω was used.

Frequency Tuning

One of the ways to realize cold tuning of the QWR is to press the beam port azimuthally, reducing the gap length. The advantage of this method is that the frequency change

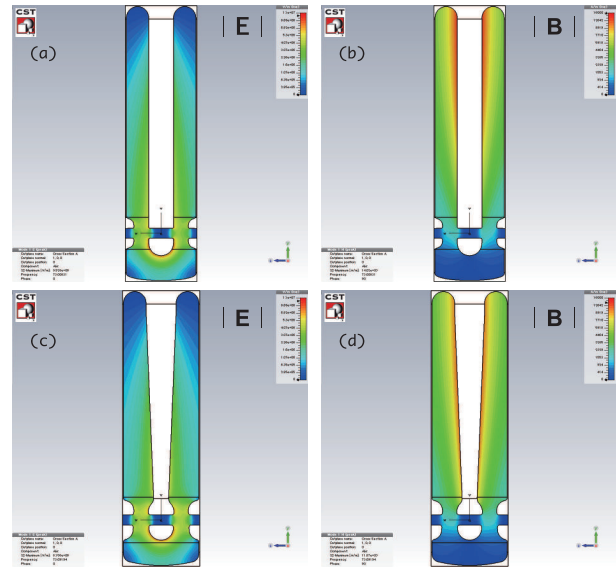


Figure 4: Contour plot of electric (a,c) and magnetic (b,d) fields for two types of SC-QWRs with a stored energy of 1 J. Plots are all to the same scale. Figures (a) and (b) are the old type and (c) and (d) are the new design.

is sensitive to the gap length. A mechanical structure acts on the beam port flange and changes the gap directly. However, installation space between resonators is limited because the resonators are placed as close as possible because the beam dynamics requires strong transverse defocusing at the acceleration gap. The other way to change the gap length is to squeeze the outer cylinder perpendicular to the beam axis [10].

Mechanical simulations of these two methods have been performed. The simulated deformation using ANSYS15.0.7 is shown in Fig. 5. In the simulation model, the thickness of the resonator wall is 4 mm. For physical properties of the Nb at 4.5 K, a Young's modulus of 125 MPa

Table 1: Characteristics of SC-QWRs for the RIKEN SC-LINAC

Frequency at 4.5 K [MHz]	73.0
β_{opt}	0.08
E_{acc} [MV/m]	4.5
E_{peak}/E_{acc}	6.0
B_{peak}/E_{acc} [$\frac{mT}{MV/m}$]	9.5
R_{sh}/Q_0 [Ω]	718
V_{acc} at $E_{acc}=4.5$ MV/m, $\beta=0.08$	1.43
G [Ω]	22.6
P_0 [W]	4.0
Inner diameter [mm^ϕ]	300
Height [mm]	1090
Aperture (beam tube) [mm^ϕ]	40.0
Q_0	8.9×10^8
Q_{ext}	1.2×10^6
Max. beam loading [kW]	1.3

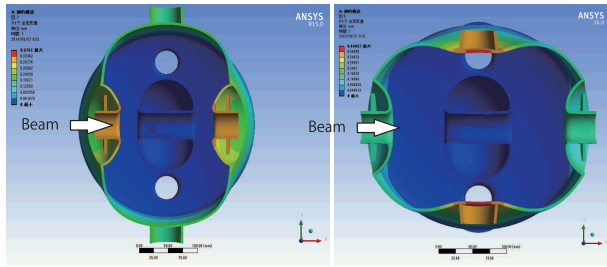


Figure 5: Frequency tuning by pressing the resonator wall.

and a Poisson ratio of 0.38 are used. The rigidity of the helium vessel is not taken in account. The left and right figures are for pressing the beam ports and pressing perpendicular to the beam axis, respectively. To press the resonator wall perpendicular to the beam axis a set of cylinders (side cylinders) is used. The vertical position of the attached cylinders is at the same height as the beam ports. A load of 5,000 N is applied to the beam ports or side cylinders. The deformations and the resulting the frequency shifts (Δf) are summarized in Table 2. The bracketed values in Table 2, obtained using MPHYSICS software from CST, which is a 3-D simulation of thermal and mechanical stress analysis, are shown to indicate the consistency between results from different simulation codes. The frequency tuning range must be set so that the maximum stress does not exceed the yield stress at 4.5 K with a mechanical safety factor. The maximum stress can be reduced further by adding ribs or modifying the corner radius between the connected parts.

Table 2: Simulation of Deformation of the Cold Tuner

Load	Beam Ports	Side Cylinders
Max. Deform. [mm]	0.375(0.380)	0.448(0.450)
Max. Stress [MPa]	116(123)	205(233)
Δf [kHz]	-9.40	6.23
Sensitivity [kHz/mm]	-24.75	13.84

Correction of Steering Effect by RF Magnetic Field

Due to the vertical asymmetry of the QWR structure, the accelerated beams are kicked downward by the RF magnetic field. To counteract this steering effect it is proposed to have a tilt between the faces of neighboring drift tubes [11]. This modification of the drift tube shape produces a vertical component in the electric field to correct the steering of the accelerated beams. To choose the tilting angle, beam orbits were obtained numerically (Runge-Kutta-Gill method) for electric and magnetic RF fields with tilting angles θ_c . The simulation was made for the first cryomodules because the steering effect is significant for low beta particles. The RF fields were obtained by interpolating the gridded data from MWS with third order spline functions. As shown in Fig. 6, $\theta_c = 2.3^\circ$ minimizes the vertical shift due to steering effect at the exit of the cryomodule.

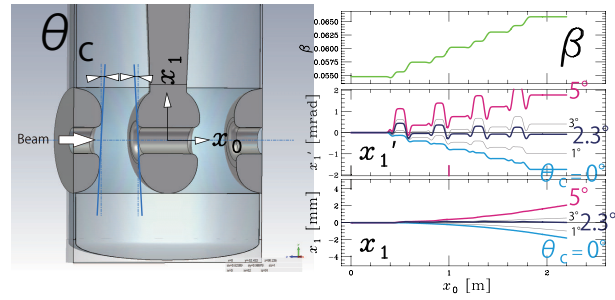


Figure 6: Orbit of center particles accelerated by the first cryomodule which contains four resonators. The angle θ_c is the tilt between opposing faces of the drift tubes.

Beam Loading Simulation

A simulation of RF power with beam loading was made via a lumped circuit model. The resonator equivalent circuit model with beam loading shown in Fig. 7 was used. In the figure, Q is the quality factor of the unloaded resonator, i_{beam} is the fundamental Fourier component of the beam current (in this case $i_{beam} = -2 \times I_{beam} \times TTF$), i_{gen} is the current output of the generator, V^{gen} is the output voltage of the generator, Z_0 is the output impedance of the generator (50Ω), Z_{in} is the input impedance seen from the coupler, Z_{cav} is the impedance of the cavity (resonator), i_{FPC} is the forward current through the capacitive coupler, i_{cav} is the current flowing into the resonator, V_{cav} is the resonator voltage and i^{load} is the reflected current flowing into the dummy load. By adjusting the capacitance of the FPC (C_{FPC}) zero reflection current can be obtained. In this case, a power output from generator and the sum of the power dissipation of the resonator wall and the beam loading become balanced. Q_{ext} is determined by the ratio of RF power transmitted into the FPC to the power stored in the resonator and depends on C_{FPC} . The loaded quality factor Q_{loaded} is obtained from the resonance curve of the stored energy with no beam loading as the ratio of the resonant frequency to FWHM and then Q_{ext} is extracted from the relation $1/Q_{loaded} = 1/Q_0 + 1/Q_{ext}$. The obtained values of Q_{ext} are plotted in Fig. 8.

The beam-loading effect can be simulated by an additional current source i^{beam} , as shown on the right-hand side

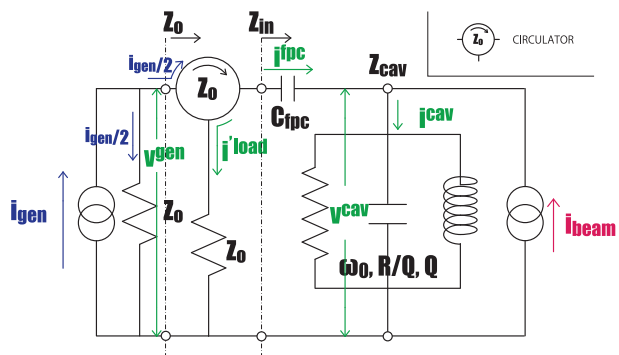


Figure 7: Equivalent circuit with beam loading.

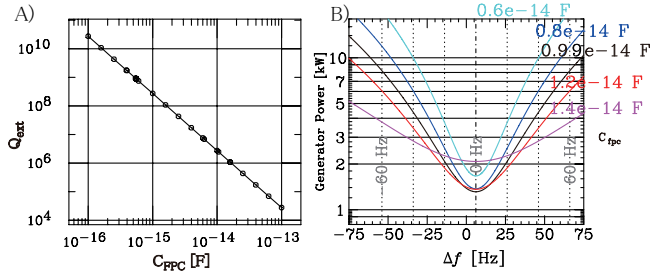


Figure 8: A) Q_{loaded} is plotted as a function of the capacity of the FPC. B) Required RF power is calculated as a function of resonator detuning Δf for various FPC capacitances, C_{FPC} .

of Fig.7. Here the beam frequency was assumed to be a sub-harmonic of the RF frequency. With beam loading, the RF current which flows into the resonator i^{cav} is represented as sum of the currents:

$$i^{\text{cav}} = i_{\text{gen}}^{\text{cav}} + i_{\text{beam}}^{\text{cav}}.$$

The currents $i_{\text{gen}}^{\text{cav}}$, $i_{\text{beam}}^{\text{cav}}$ are obtained according to Kirchhoff's law. The amplitude and phase of the output current of the generator i_{gen} is controlled so that the amplitude of the cavity voltage and its phase ϕ_s with respect to the beam phase stay constant:

$$\begin{aligned} V_{\text{gen}}^{\text{cav}} &= Z_{\text{cav}} \cdot i_{\text{gen}}^{\text{cav}} \\ &= V^{\text{cav}} \cdot \exp(j\phi_s) - V_{\text{beam}}^{\text{cav}} \\ i_{\text{gen}} &= \frac{Z_0 + Z_{\text{FPC}} + Z_{\text{cav}}}{Z_0} \cdot i_{\text{gen}}^{\text{cav}}. \end{aligned}$$

The output RF powers of the power source are calculated as $P_{\text{gen}} = \text{real}(V_{\text{gen}}^{\text{cav}} \cdot i_{\text{gen}}^{\text{cav}*})/2 = Z_0 \cdot |i_{\text{gen}}|^2/2$ and are plotted as a function of the difference between RF frequency and resonant frequency for various values of C_{FPC} in Fig.8. Here a^* denotes a complex conjugate of a .

External Q of the Fundamental Power Coupler

To determine the tuning stroke of the antenna of the FPC, Q_{ext} is calculated as a function of the coupler antenna insertion. Values of Q_{ext} are obtained according to the method proposed by Balleyguier [12]. Following this method, the ratio of the volume integral of $|E|^2(H^2)$ to the surface integral of $|E|^2(|H|^2)$ at the port set at the end of the FPC (see Fig. 9) gives Q_{ext} :

$$\begin{aligned} Q_{\text{ext}} &= Q_1 + Q_2 \\ &= \frac{\omega_1}{c} \frac{\iiint_{\text{cavity}} |E_1|^2 dV}{\iint_{\text{port}} |E_1|^2 dS} + \frac{\omega_2}{c} \frac{\iiint_{\text{cavity}} |H_2|^2 dV}{\iint_{\text{port}} |H_2|^2 dS}. \end{aligned}$$

The suffixes 1 and 2 indicate that calculations were made with the boundary conditions at the port being open and short, respectively. As plotted in Fig. 9, a ± 5 mm stroke of the coupling antenna changes Q_{ext} by a factor of 10.

SRF Technology - Cavity

E02-Non-elliptical design

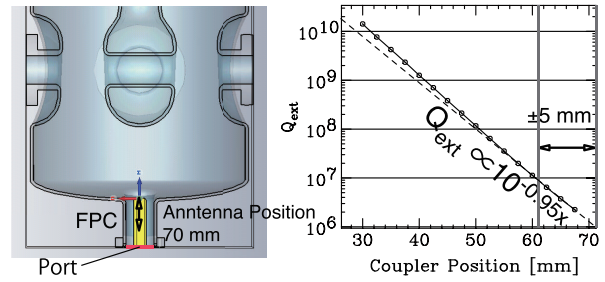


Figure 9: Model for MWS simulation (left) and Q_{ext} plotted as a function of the position of the coupler antenna (right).

PROTOTYPE

Prototyping of the SC-QWR for low β heavy-ions such as deuteron, alpha, carbon started this year. A design study of a SC-QWR and its test cryomodule is also in progress. Fabrication of the first SC-QWR will be completed in Q1 of 2016 and vertical tests will subsequently be conducted. The project plans to make acceleration tests of very intense beams with an energy of 6 MeV/u from the RIKEN linac booster [13].

Design of the Prototype Resonator

The frequency of the resonator is chosen to be 75.5 MHz, which is the frequency of the RIKEN linac booster. The shape of the resonator for the RIKEN SC-LINAC, whose frequency is 73.0 MHz, was modified to meet this requirement.

Cross-sectional views of the prototype resonator are shown in Fig. 10. The shape of the resonator was modified considering not only local stresses caused by atmospheric pressure and pressing by the tuner but also convenience of fabrication. The prototype will be manufactured from pure Nb (residual resistivity ratio, RRR > 250) sheets with a thickness of 4 mm. The end drift tubes, stem, upper toroidal part, bottom cover and the outer cylinder will

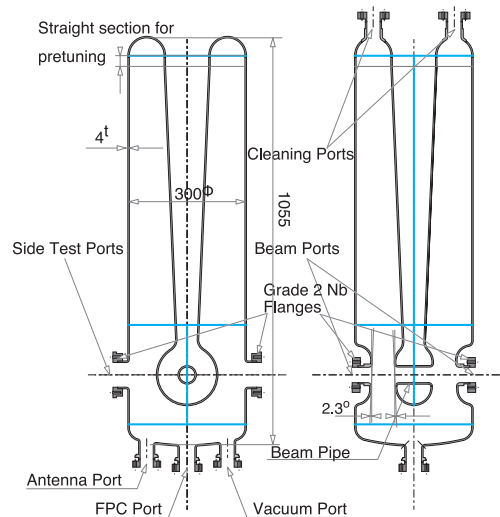


Figure 10: Cross-sectional views of the prototype resonator.

ISBN 978-3-95450-178-6

979

be formed by deep drawing and joined by electron-beam welding (EBW) [14]. In Fig. 10, blue lines indicate boundaries between these parts. The faces of the drift tubes are tilted by 2.3° . Pre-tuning is supposed to be done by cutting the straight section of the stub and the outer cylinder.

The prototype resonator has 9 ports. The two ports on the upper toroidal part are cleaning ports. The center port at the bottom is for the FPC and the other two ports are for pickup antennas. In the median plane, the resonator is equipped with two beam ports and two test ports. The test ports are for future R&D of a plunger type tuner. As the material for the flanges of these ports Grade-2 Nb is chosen instead of NbTi, and flanges utilizing HELICOFLEX gaskets are used for the vacuum seal. After the vertical tests of the resonator, a He jacket made of Ti, whose thermal expansion coefficient is similar to that of Nb, will be mounted by EBW.

Mechanical Study of the Resonator

Investigation of the rib structure mounted on the upper toroidal part to suppress the vertical deformation and mechanical vibration of the stem (pendulum modes) is now in progress. The QWR resonator has pendulum vibration modes that are azimuthal (mode 1) and perpendicular to the beam (mode 2). Table 3 summarizes estimates made by ANSYS of deformation with a uniform pressure of 0.1313 MPa and the frequencies of vibration modes with and without a rib structure (Fig. 11) similar to that of the SPIRAL2 $\beta = 0.07$ resonator [10]. The maximum deformation occurs at the inward edge of the flanges of the two clean ports on the upper toroidal part which incline inwardly in the radial direction accompanied with a downward displacement of the stem. As the model number indicated in the first row of Table 3 increases, stiffness increases and deformation becomes smaller. Also the stiffer the toroidal part, the higher the frequency of the vibration modes becomes. It is crucial to avoid the situation in which the frequency of the vibration mode is 50 Hz which matches the frequency of commercial electric power.

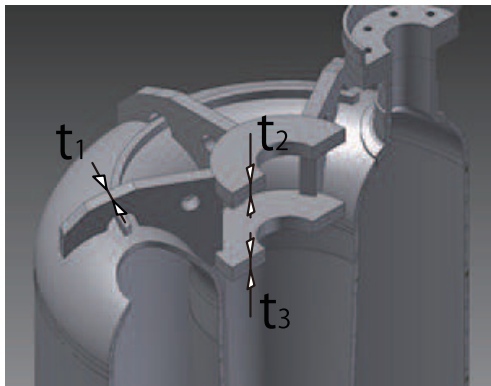


Figure 11: Rib structure for the upper toroidal part of the prototype resonator.

Table 3: Deformation and the Frequencies of Vibration Modes Estimated by ANSYS Simulation

Model	t1 mm	t2 mm	t3 mm	δZ mm	f_{mode1} Hz	f_{mode2} Hz
1	no	no	no	0.254	32.5	33.5
2	5	5	5	0.073	45.7	47.2
3	5	10	10	0.067	48.2	49.4
4	10	10	10	0.051	54.3	55.2

Surface Treatment

The 9 ports of the resonator will be utilized for surface cleaning. The planned surface treatment procedure is

Light BCP \rightarrow HPR \rightarrow Annealing \rightarrow BCP \rightarrow HPR.

With the second BCP process we will try to pre-tune to the resonant frequency. For the HPR process a new system dedicated to the QWRs will be installed in the class 1 clean room [15].

Cryostat

A plan view of the test cryomodule is shown in Fig. 12. The resonator vacuum must be separate from the vacuum of the cryostat chamber to maintain the high cleanliness of the resonator surface. The FPCs have a variable coupling mechanism that can be tuned without warming up the cold mass or breaking the vacuum of the cryostat. A room temperature magnetic shield is employed to minimize the effects of geomagnetism. The single-stage thermal shield is designed to be cooled by using a small cryo-cooler. To minimize the heat flow into the 4 K cold mass and the thermal shield from the parts at room temperature, transition parts are attached to beam pipes and the outer conductors of the FPCs.

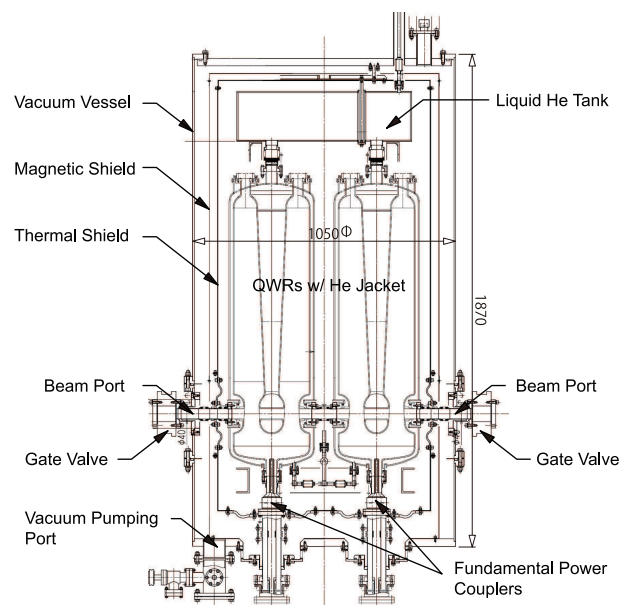


Figure 12: Plan view of the test cryomodule.

Table 4: Thermal Flow Estimation [W/resonator]

Temperature	Kind	4K	40K
Resonator	Dynamic	3.84	-
Coupler	Conduction	0.36	8.13
	Radiation	0	-
	Dynamic	0.14	1.19
Beam pipe	Conduction	0.06	0.99
Thermal shield	Radiation	0.01	1.64
He pipes	Conduction	0.35	-
Support	Conduction	0.19	2.95
Sensor cables	Conduction	0.08	0.06
Total		5.03	14.96

The dynamic and static heat loads from the FPC were estimated using MWS and MPHYSICS. The estimated thermal flow is summarized in Table 4. The values in this table are based on the following assumptions. The FPCs are coaxial and handle a maximum RF power of 10 kW. Double vacuum windows are adopted. The antennas of the FPCs are made of bulk copper and are cooled by heat conduction through the cold window. The outer conductor is made of copper-plated stainless steel and its RRR is assumed to be 30. The placement of the warm and cold ceramic disk-type windows and the thermal anchors are optimized [16]. Since the optimum placement of the ceramic windows and thermal anchor is sensitive to the effective RRR of copper-plated conductors, it is important to know the RRR of the real material before the placement is decided. The design of the mechanical structure to deform the resonator wall in the azimuthal direction has not yet been completed. So the heat load from mechanical tuner is not included in the estimation.

SUMMARY

The construction of a superconducting linac to upgrade the intensity of uranium beams at the RIKEN RIBF has been proposed. Design studies for a superconducting cryomodule for the low β section, including the QWR, fundamental power coupler and cold tuner, have been conducted. This year the prototyping of an SC-QWR for a very intense ion accelerator was started. Manufacturing of the QWR is in progress and the vertical test of the resonator is planned for March 2016. A test cryomodule which is capable of containing two resonators will be manufactured in 2016 and a cool down test will be performed in March 2017.

ACKNOWLEDGEMENT

Development of a prototype superconducting resonator and its cryomodule was funded by the ImPACT Program of the Council for Science, Technology and Innovation (Cabinet Office, Government of Japan).

REFERENCES

- [1] Y. Yano, Nucl. Instrum. and Meth., **B261**(2007)1009.
- [2] N. Sakamoto, "Performance of New Injector RILAC2 for RIKEN RI-BEAM Factory", LINAC'14, Geneva, September 2014, THPP116, p. 1123.
- [3] K. Suda et al., Nucl. Instrum. and Meth., **A277**(2013)55.
- [4] K. Yamada, "Beam Commissioning and Operation of New Linac Injector for RIKEN RI-beam Factory", IPAC'12, New Orleans, May 2012, TUOBA02, p. 1071.
- [5] Y. Yano, "Recent Achievements at the RIKEN Ring Cyclotron", Cyclotrons'92, Vancouver, July 1992, I-21, p. 102.
- [6] N. Fukunishi, "Heavy-ion Cyclotron Gymnastics and Associated Beam Dynamics Issues", HB2014, East Lansing, November 2014, MOZLR09, p. 18.
- [7] K. Yamada et al., "Conceptual Design of SC Linac for RIBF-Upgrade Plan", SRF2013, Paris, September 2013, MOP021, p. 137.
- [8] K. Yamada et al., "Design of a New Superconducting Linac for the RIBF Upgrade", LINAC'14, Geneva, September 2014, THPP118, p. 1127.
- [9] <http://www.cst.com>.
- [10] G. Devanz et al., "SPIRAL2 Resonators", SRF2005, Ithaca, July 2005, MOP02, p. 108.
- [11] P. N. Ostroumov and K.W. Shepard, Phys. Rev. ST. Accel. Beams **4**(2001)110101.
- [12] P. Balleyguier, "External Q Studies for APT SC-Cavity Couplers", LINAC'98, Chicago, August 1998, MO4037, p. 133.
- [13] O. Kamigaito et al., Rev. Sci. Instr. **76**(2005)013306.
- [14] T. Yanagisawa et al., "Status of Superconducting Quarter Wave Resonator Development at MHI", HIAT'15, Yokohama, September 2015, WEPB17.
- [15] A. Miyamoto et al., "MHI's Production Activities of Superconducting Cavity", SRF 2015, THPB029.
- [16] K. Ozeki et al., "Design of Input Couple for RIKEN Superconducting Quarter-wave-length Resonator", SRF 2015, THPB084.